

Detergent-resistant microdomains mediate activation of host cell signaling in response to attaching–effacing bacteria

Grace Shen-Tu^{1,2}, David B Schauer^{3,*}, Nicola L Jones^{1,4,5} and Philip M Sherman^{1,2,4,6}

Enterohemorrhagic *Escherichia coli* (EHEC) O157:H7 causes outbreaks of bloody diarrhea and the hemolytic–uremic syndrome. EHEC intimately adheres to epithelial cells, effaces microvilli and induces attaching–effacing (AE) lesions. Detergent-resistant microdomains (lipid rafts) serve as membrane platforms for the recruitment of signaling complexes to mediate host responses to infection. The aim of this study was to define the role of lipid rafts in activating signal transduction pathways in response to AE bacterial pathogens. Epithelial cell monolayers were infected with EHEC (MOI 100:1, 3 h, 37°C) and lipid rafts isolated by buoyant density ultracentrifugation. Phosphoinositide 3-kinase (PI3K) localization to lipid rafts was confirmed using PI3K and anti-caveolin-1 antibodies. Mice with cholesterol storage disease Niemann–Pick, type C were used as *in vivo* models to confirm the role of lipid rafts in mediating signaling response to AE organisms. In contrast to uninfected cells, PI3K was recruited to lipid rafts in response to EHEC infection. Metabolically active bacteria and cells with intact cholesterol-rich microdomains were necessary for the recruitment of second messengers to lipid rafts. Recruitment of PI3K to lipid rafts was independent of the intimin (*eaeA*) gene, type III secretion system, and production of Shiga-like toxins. Colonization of NPC^{-/-} colonic mucosa by *Citrobacter rodentium* and AE lesion formation were both delayed, compared with wild-type mice infected with the murine-specific AE bacterial pathogen. *C. rodentium*-infected NPC^{-/-} mice had reduced colonic epithelial hyperplasia (64 ± 8.251 vs 112 ± 2.958 μm ; $P < 0.05$) and decreased secretion of IFN- γ (17.6 ± 17.6 vs 71 ± 26.3 pg/ml, $P < 0.001$). Lipid rafts mediate host cell signal transduction responses to AE bacterial infections both *in vitro* and *in vivo*. These findings advance the current understanding of microbial–eukaryotic cell interactions in response to enteric pathogens that hijack signaling responses mediated through lipid rafts.

Laboratory Investigation (2010) 90, 266–281; doi:10.1038/labinvest.2009.131; published online 7 December 2009

KEYWORDS: colonic epithelial cell hyperplasia; enterohemorrhagic *Escherichia coli* O157:H7; *Citrobacter rodentium*; lipid rafts; microbial–host interaction; phosphoinositide 3-kinase

Escherichia coli is a facultative Gram-negative bacterium normally present in commensal colonic microflora. However, some *E. coli* strains possess specific virulence factors enabling them to cause disease in mammalian hosts.¹ Enterohemorrhagic *Escherichia coli* (EHEC) O157:H7 is responsible for outbreaks of diarrhea, hemorrhagic colitis and the hemolytic–uremic syndrome (HUS), which is the most common cause of acute renal failure in children.² For instance, an *E. coli* O157:H7 outbreak in North America was reported in

the fall of 2006 initiated from the ingestion of contaminated, prepackaged spinach.³

Several virulence factors are thought to mediate disease pathogenesis. EHEC produces a potent cytotoxin known as Verotoxin (Shiga-like) toxin.⁴ Verotoxin is an AB₅ subunit toxin that binds to globotriaosylceramides (Gb₃) that are localized in membrane lipid rafts of host cells,⁵ inactivates 28S ribosomal RNA to disrupt protein synthesis, and promotes apoptosis, leading to epithelial cell death.⁶

¹Research Institute, Hospital for Sick Children, University of Toronto, Toronto, ON, Canada; ²Institute of Medical Science, University of Toronto, Toronto, ON, Canada; ³Division of Comparative Medicine, Department of Biological Engineering, Massachusetts Institute of Technology, Cambridge, MA, USA; ⁴Department of Paediatrics, University of Toronto, Toronto, ON, Canada; ⁵Department of Physiology, University of Toronto, Toronto, ON, Canada and ⁶Laboratory Medicine & Pathobiology, University of Toronto, Toronto, ON, Canada

Correspondence: Dr PM Sherman, MD, FRCPC, Department of Paediatrics, Hospital for Sick Children, Room 8409, 555 University Avenue, Toronto, Ontario, Canada M5G 1X8.

E-mail: philip.sherman@sickkids.ca

*Deceased.

Received 18 April 2009; revised 27 October 2009; accepted 29 October 2009

EHEC O157:H7 infection is also characterized by intimate bacterial attachment to epithelial cells mediated through a variety of adherence factors.⁷ *E. coli*-secreted proteins, encoded on a 35-kilobase pathogenicity island referred to as the locus of enterocyte effacement (LEE), are injected into the cytosol of infected cells through a type III secretion system-encoded molecular syringe.⁸ The translocating intimin receptor (Tir), also known as EspE, functions as a receptor for the *eae* gene-encoded bacterial outer membrane protein, intimin.⁹ Tir–intimin interactions give rise to intimate attachment of EHEC O157:H7 to eukaryotic cells and the recruitment of host actin cytoskeleton elements, which form dense adhesion pedestals and the effacement of intestinal brush-border microvilli, collectively known as the attaching–effacing (AE) lesion.¹

Citrobacter rodentium is a naturally occurring mouse-specific noninvasive bacterial pathogen that is genetically related to EHEC, because it also uses AE lesion formation as a mechanism of infection and colonization of the colon. Genes encoding the ability of both *C. rodentium* and EHEC to induce AE lesions are located on the LEE pathogenicity island. *C. rodentium* infection of mice causes colonic epithelial hyperplasia that resolves spontaneously by post-infection day 28.¹⁰

The effector protein Tir is inserted into cholesterol- and sphingolipid-enriched microdomains in the eukaryotic cell plasma membrane bilayer, referred to as lipid rafts.^{11,12} Cholesterol is an important component of eukaryotic cellular membranes, which is known to dynamically associate with sphingolipids to form heterogeneous microdomains (lipid rafts).¹³ These cholesterol-enriched microdomains serve as platforms for the recruitment of cell signaling complexes to a microenvironment in which they are sheltered from nonraft enzymes that can interfere with signaling processes.^{13,14} Lipid rafts contribute to a variety of functions in eukaryotic cells, including cell signaling, trafficking, and protein sorting.^{15,16}

The aim of this study was to determine whether AE bacterial infections promote the recruitment of phosphoinositide 3-kinase (PI3K) to lipid rafts and determine the role of these microdomains in disease pathogenesis.

MATERIALS AND METHODS

Tissue Culture Cell Lines

The HEP-2 human laryngeal epithelial cell line (CCL23; American Type Culture Collection, Manassas, VA, USA) and Intestine 407 embryonic intestinal cells (CCL-6; ATCC) were used as model systems *in vitro*. HEP-2 cells were cultured at 37°C in 5% CO₂ in minimal essential medium (MEM) supplemented with 10% fetal bovine serum, 1% sodium bicarbonate, 1% Fungizone, and 1% penicillin-streptomycin. Intestine 407 cells were cultured in MEM supplemented with 10% fetal bovine serum and 2% penicillin–streptomycin (all media and supplemental reagents from Life Technologies, Grand Island, NY, USA).

Bacterial Strains and Growth Conditions

The bacterial strains used in this study are shown in Table 1. EHEC O157:H7, strain CL56 and *E. coli* O113:H21, strain CL15 were stored at –80°C and regrown on 5% sheep blood agar plates at 4°C. Colonies were transferred from plates into Penassay broth and incubated at 37°C for 18 h and then regrown for 3 h in an antibiotic-free tissue culture medium at 37°C for mid-log phase. Heat-killed bacteria were prepared by boiling mid-log phase bacteria at 100°C for 30 min. Formalin-fixed bacteria were washed with phosphate-buffered saline (PBS) and treated with formaldehyde (12%) for 6–8 h at 4°C.

Before infection of tissue culture cells, bacteria were washed with PBS and resuspended in antibiotic-free MEM. For chloramphenicol treatment, mid-log phase bacteria were pelleted and resuspended in chloramphenicol (100 µg/ml) for 6–8 h at 4°C.¹⁷ Bacteria were added to epithelial cells grown in 10 cm diameter tissue culture dishes (Starstedt, Montreal,

Table 1 Bacterial strains and treatments used in the *in vitro* studies

<i>Escherichia coli</i> strains	Treatment	Description	Source	Reference
CL56 (EHEC O157:H7)	Boil at 100°C for 30 min	Non-viable bacteria with disrupted structure	HC, HUS	2,17
	Chloramphenicol	Stop the bacterial protein synthesis		
	Formaldehyde	Kill the bacteria but keeping the structure intact		
CL15 (O113:H21)	—	Without the LEE pathogenicity island	HC, HUS	38
86-24	—	Wild-type EHEC	HC, HUS	17
CVD451	—	Type III secretion-deficient mutant of parental strain 86-24	Lab	17
85-289	—	Wild-type EHEC	HC, HUS	17
85-170	—	Stx1 and Stx2 negative mutants of parental strain 85-289	Lab	17

Abbreviations: HC, hemorrhagic colitis; HUS, hemolytic uremic syndrome.

The various strains of *E. coli* and related mutants were grown overnight on sheep blood agar from frozen stocks in 37°C and subsequently grown in Penassay broth overnight. The overnight growth in broth was used to infect model cell lines to delineate microbial–host cell interaction through signaling cross-talk.

Que., Canada), at a multiplicity of infection of 100 bacteria to one eukaryotic cell, for 1 h at 37°C in antibiotic-free MEM. Uninfected cells were used as a negative control. After 1 h of infection, cells were washed with PBS (pH 7.0) to remove nonadherent bacteria.

Cultured Supernatant and Conditioned Medium Preparation

To collect bacterial culture supernatants, 10 ml of EHEC O157:H7 grown in Penassay broth was centrifuged at 3000 r.p.m. for 15 min and the supernatant was filtered using a 0.45 µm filter into a new tube for storage at -20°C until use. To collect conditioned medium, EHEC O157:H7 strain CL-56 grown overnight in 10 ml Penassay broth (37°C) was used to infect monolayers of HEp-2 cells (MOI 100:1). After 1 h, the medium was centrifuged (3000 r.p.m., 15 min), and 30 ml of conditioned medium was pooled together and concentrated using a 3 kDa Amicon Ultrafilter (Millipore). Unfiltered conditioned medium was collected using centrifugation and 100 µg/ml of chloramphenicol was added to halt bacterial protein synthesis.

C. rodentium, strain DBS100 (ATCC 51459) was stored in Luria Bertani (LB) broth with 50% glycerol at -80°C. Bacteria were grown from frozen stocks on LB agar plates at 37°C and stored at 4°C for no more than 2 weeks. Bacteria were inoculated into 10 ml LB broth and grown at 37°C overnight. Before infection of mice, overnight cultures were centrifuged at 3000 r.p.m. for 10 min and resuspended in 2.5 ml of LB broth to obtain a concentration of 10¹⁰ bacteria per ml.

Whole-Cell Protein Extraction

HEp-2 cells were infected either with *Escherichia coli* O157H7 or with *C. rodentium* for 1, 3, and 6 h. Cells were washed thrice with ice-cold PBS (pH 7.0) and whole-cell protein extracts were collected for storage at -80°C, as previously described.¹⁸

Depletion of Cholesterol using Methyl-β-Cyclodextrin (MβCD)

HEp-2 cells were treated with MβCD (Sigma Chemical, St Louis, MO, USA) (1–10 mM) to disrupt cholesterol-enriched microdomains by chelating plasma membrane cholesterol.¹⁹ Before bacterial infection, epithelial cells were incubated with MβCD (10 mM) in antibiotic-free MEM for 1 h at 37°C. The medium was aspirated off cell monolayers and washed with PBS before bacterial infection.²⁰

Treatment with Pharmacological Inhibitors

Tissue culture cells were preincubated with either the phosphoinositide-3 kinase inhibitor LY294002 (100 µM; Sigma Chemical) or with an equal concentration of the inactive analog LY303511 for 1 h at 37°C.²¹ After removal of the inhibitor, cells were rinsed with PBS and infected with bacteria for 1 h at 37°C.

Isolation of Detergent-Resistant Membranes

Infected epithelial cells were scraped and pelleted in 4 ml of sterile PBS in 15 ml conical tubes. Cells were then lysed with 0.8 ml TN buffer (25 mM tris-HCl pH 7.5, 150 mM NaCl, 1 mM DTT, 10% sucrose, 1% Triton X-100, leupeptin, 2 µg/ml pepstatin A, 10 µg/ml aprotinin, 0.5 mM PMSF, 1 mM Na₃VO₄) for 30 min on ice. The samples were then mixed with 1.7 ml of Optiprep (Axis-Shield PoC AS, Oslo, Norway) and transferred into SW41 centrifuge tubes (Beckman Instruments, Palo Alto, CA, USA). Optiprep (60%) was diluted with TN buffer to produce 35 and 5% solutions (adapted from references²² and²³), which were then layered on top of samples and centrifuged at 160 000 × g for 20 h at 4°C. Eight 1.5 ml fractions were then collected from top to bottom of the gradient generated by ultracentrifugation.²⁴

Immunoblotting

Aliquots (10 µl) of each fraction were analyzed for PI3K and caveolin-1. Proteins were separated by precast 10% Tris-HCl (Biorad) sodium dodecyl sulfate polyacrylamide gel electrophoresis (SDS-PAGE) with a protein ladder standard (BioRad, broad molecular range ladder) at 120 V for 1–1.25 h at room temperature. After electrophoresis, proteins were transferred onto nitrocellulose membranes (Pall Corporation, Pensacola, FL, USA) at 100 V for 1.5 h at 4°C and incubated in Odyssey blocking buffer (LI-COR Biosciences, Lincoln, NE, USA) for 0.5–1 h at 20°C. Blocking buffer was then decanted off and membranes were probed with anti-caveolin-1 as a lipid raft marker protein (Santa Cruz Biotechnology, CA, USA; 1:1000) and with primary antibodies against PI3K p85 (Upstate Biotechnology, Lake Placid, NY, USA; 1:1000) overnight at 4°C on a shaker. Whole-cell extracts were probed with native- and phospho-Akt antibody (Cell Signaling, Beverly, MA, USA; 1:1000 dilution). After washing the membrane four times with PBS and 0.1% Tween (5 min per wash), IRDye 800 goat anti-rabbit immunoglobulin G (IgG) secondary antibody (Rockland Immunochemicals, Gilbertsville, PA, USA; 1:20 000) was added and incubated for 1 h at room temperature on a shaker. The blots were then washed four times with PBS and 0.1% Tween and once with PBS alone. The membrane was then scanned using the Odyssey system (LI-COR Biosciences) with the 800 nm channel. The integrative intensity of the detected bands was obtained using software provided with the infrared imaging system (LI-COR Biosciences). Western analysis was performed on collected whole-cell lysates probed with both Akts (Cell Signaling, Denver, MA, USA; 1:1000 dilution).

Immunostaining

HEp-2 cells were grown to subconfluency and treated with MβCD (10 mM; Sigma Chemical) for 1 h at 37°C. To add cholesterol back into cholesterol-depleted cells, 200 µg/ml of soluble cholesterol (Sigma) in an antibiotic-free medium was added to cells for 45 min at 37°C. After depletion–repletion of cholesterol, cells were washed with PBS, fixed in 3.7%

paraformaldehyde, and permeabilized with 0.1% Triton X-100. Lipid rafts were visualized using Alexa Fluor 594-labeled cholera toxin subunit B (Invitrogen, Carlsbad, CA, USA).²⁵

Animals

BALB/c mice ($n=5$ for 6 days uninfected and *C. rodentium* infected; $n=5$ for 12 days uninfected and *C. rodentium* infected) and homozygous BALB/cNctr-npc1^{m1N/m1N} (*Npc1*^{-/-}) mice ($n=4$ for 6 days uninfected and *C. rodentium* infected; $n=4$ for 12 days uninfected and *C. rodentium* infected) with Niemann–Pick type C disease were obtained from Jackson Laboratory (Bar Harbor, ME, USA) at 4–5 weeks of age, before the onset of a progressive neurological disorder.²⁶ Animals were housed in microisolate cages in a containment unit and were allowed free access to water and chow. All animal experiments were carried out after review and approval by the Laboratory Animal Services, Hospital for Sick Children, Toronto, ON, Canada.

Infection of Mice with *C. rodentium*

Mice were inoculated orogastrically with either 10^9 *C. rodentium* in 100 μ l LB broth, or sham infected with an equal volume of LB broth alone, and then followed up for 6–12 days.¹⁰ Mice were monitored for bacterial shedding using rectal swabs streaked onto MacConkey lactose agar plates.²⁷

Tissue Collection

At necropsy, spleens and colonic sections were harvested for further experimental analyses. Spleens were placed into 4 ml of RPMI tissue culture medium and kept on ice. Segments (~5 mm in length) of distal colon were placed into Universal fixative (4% paraformaldehyde, 1% glutaraldehyde in 0.1 M phosphate buffer) for further processing by electron microscopy.²⁸ Segments from the remainder of the distal colon were placed in 10% neutral-buffered formalin and processed for histological assessment. In some experimental groups, mice were injected intraperitoneally with a 10 mg/ml 5-bromo-2'-deoxyuridine (BrdU; Sigma) solution in PBS at a concentration of 5 μ l/g 1 h before being killed. Mice injected with BrdU were not used to prepare splenocytes.

Histology and Immunohistochemistry

Formalin-fixed tissues were embedded in paraffin, sectioned at 5–7 μ m, and mounted onto positively charged microscope slides for further processing. For histology, slides were rinsed in distilled water and stained with Mayer's hematoxylin for 15 min. Excess stain was removed by rinsing in water and sections were fixed by rinsing five times in ammonia water. Slides were then rinsed in 95% ethanol and counterstained in eosin for 3 min.

To detect *C. rodentium* bound to intestinal mucosal surfaces using immunohistochemistry, mounted tissue sections were baked overnight at 60°C, dewaxed in xylene, and hydrated to distilled water through decreasing concentrations of ethanol. The immunohistochemical procedure was per-

formed on an auto-immunostainer (NEXES, Vetana Medical Systems, Tuscon, AZ, USA). Rabbit polyclonal anti-*C. rodentium* diluted 1:400, as well as secondary antibody staining with biotinylated anti-rabbit IgG (Vector Laboratories, Burlingame, CA, USA) at a dilution of 1:100, was detected using a DAB (3-3'-diaminobenzidine) detection system (Ventana Medical Systems, Tuscon, AZ, USA). Slides were then counterstained with hematoxylin to provide nuclear detail.

To detect apoptotic cells, TUNEL assay for *in situ* end labeling was performed and adapted to an automated immuno/*in situ* hybridization instrument (Discovery, Ventana). Before staining, colonic sections were deparaffinized, as above, and blocked for endogenous peroxidase by Protease I (Ventana Medical Systems) digestion for 12 min. Slides were then incubated with recombinant terminal deoxynucleotidyl transferase (GIBCO BRL, Life Technologies, Grand Island, NY, USA) and biotin 16-dUTP (Roche Diagnostics Corporation, Indianapolis, IN, USA) to label the nuclei of cells undergoing programmed cell death.²⁹ Colorimetric visualization, using avidin-HRP and DAB, was performed as described above.

To detect proliferating cells within colonic crypts, colonic sections from mice injected intraperitoneally with BrdU before being killed were dewaxed and hydrated, as detailed above. Slides were then treated with pepsin digestion, acidified in 4N HCl to denature DNA, and blocked for endogenous peroxidase. Immunohistochemical staining with a mouse anti-BrdU antibody (Dako, Carpinteria, CA, USA) was performed on an auto-immunostainer (Discovery, Ventana Medical Systems) at a dilution of 1:50 using the ARK kit (Dako) to prevent mouse-on-mouse cross reactivity. Detection and visualization used a peroxidase-conjugated streptavidin secondary reagent (Dako) and a DAB chromogen substrate.

Histology and immunohistochemistry slides were viewed using a light-field microscope (Leica DM 4600B, Leica Microsystems, Richmond Hill, ON, Canada). Photomicrographs were captured using a digital camera (Leica DC 500) and analyzed using integrated software (Leica IM500 Image Manager).

Transmission Electron Microscopy

Distal colonic segments fixed in Universal fixative for 24 h were postfixed in 2% aqueous osmium tetroxide for 1 h at 20°C. Dehydration was performed in graded acetone, followed by embedding in epoxy resin. Osmium postfixation, dehydration, and embedding were conducted in a Pelco Biowave microwave oven (Pelco International, Redding, CA, USA). One-micrometer-thick sections were stained with toluidine blue and ultrathin sections were stained with uranyl acetate and lead citrate. Electron microscopy examination was performed using a transmission electron microscope (JEM 1230, Joel USA Corp., Peabody, MA, USA).

Cytokine Profiles of Splenocytes

The production of IFN- γ and IL-10 from isolated splenocytes was performed, as described previously.^{27,30} Briefly, spleens were mashed through sterile filter screens in RPMI medium to obtain single-cell suspensions. Cells were incubated in red cell lysis buffer for 3 min and washed three times. The pellet was layered with 5 ml of lympholyte-M (Cedarlanes Laboratories, Hornby, ON, Canada) and spun at 1000 r.p.m. for 10 min. Isolated cells were washed three times and resuspended in RPMI medium containing 10% fetal calf serum. Splenocytes were enumerated and equal numbers of cells were incubated with sterile *C. rodentium* whole-cell sonicate for 72 h at 37°C. IFN- γ and IL-10 cytokine levels were then measured using commercially available immunoassay kits (Medicorp, Montreal, Que., Canada), according to the manufacturer's instructions.

Data Analyses

Results are reported as means \pm standard errors of the mean (s.e.m.). To test for the significance between two groups, two-tailed Student's *t*-test was used, with $P < 0.05$ considered as statistically significant. One-way analysis of variance (ANOVA) was used for data derived from more than two study groups.³¹

RESULTS

PI3K is Recruited to Lipid Rafts in Response to Enterohemorrhagic *E. coli* Infection

After *E. coli* O157:H7 infection of HEp-2 cells, PI3K was recruited to the sucrose fraction containing caveolin-1, which was used as a lipid raft marker protein¹⁸ (Figure 1a). There was a significant increase in the amount of PI3K present in the lower density fraction of EHEC-infected cells, indicating that *E. coli* O157:H7 induced the translocation of PI3K to lipid rafts. Protein recruitment to lipid rafts was not observed when tissue culture cells were infected with heat-killed bacteria (Figure 1a), showing that recruitment of PI3K is triggered by exposure of epithelial cells to live organisms and not to bacterial surface-derived structural constituents. The increase in PI3K recruitment to lipid rafts in EHEC-infected cells was quantified by using densitometry to determine integrated intensity values (Figure 1b; $n = 5$, $P < 0.05$). Chloramphenicol-treated bacteria also markedly reduced the recruitment of PI3K to lipid rafts (Figure 1c), indicating that activation of these signal transduction cascades is caused by newly synthesized bacterial proteins.³² EHEC O157:H7 infection of Intestine 407 cells also induced activation and translocation of PI3K (Figure 1d).

PI3K Recruitment to Lipid Rafts is Independent of Known EHEC Virulence Factors

Similar to observations in EHEC O157:H7-infected cells, an increase in PI3K level in caveolin-1-enriched fraction 3 was observed in response to infection with the *eae*-negative *E. coli*, strain CL15 (VTEC O113:H21), indicating that

recruitment to lipid rafts in response to EHEC infection (Figure 1a) is independent of the AE (*eae*) gene, because strain CL15 does not contain the LEE pathogenicity island required to cause AE lesions.³³ Infection of HEp-2 cells with *E. coli*, strain CVD451, a type III secretion-deficient mutant,¹⁷ also resulted in increased recruitment of PI3K to lipid rafts (Figure 2a). Similarly, infection with *E. coli*, strain 85-170, an Stx-1 and Stx-2 negative mutant,¹⁷ also showed the recruitment of host signaling molecules to lipid rafts (Figure 2a). Taken together, these findings indicate that recruitment of signal transduction molecules to lipid rafts is independent of the bacterial type III secretion system and the production of Shiga-like toxins 1 and 2.

Recruitment of PI3K to Lipid Rafts is Blocked by a Specific PI3K Inhibitor

Recruitment of PI3K in response to EHEC O157:H7 infection was reduced in cells pretreated with the PI3K inhibitor, LY294002 (100 μ M), by 40% (relative to EHEC-infected alone), but not when an equal concentration of an inactive analog (LY303511) was used (integrated intensity readings of the PI3K band in immunoblots, relative to caveolin-1, were 0.805 for LY294002-treated cells, 1.229 for LY303511-treated epithelia and 1.332 for EHEC-infected cells) (Figure 2b). DMSO alone, tested as a vehicle control, did not result in a reduction in PI3K recruitment to lipid rafts (data not shown). These findings support the hypothesis that activated PI3K is recruited to lipid rafts in response to EHEC infection.³⁴

M β CD Blocks PI3K Recruitment to Lipid Rafts in Response to EHEC Infection

To confirm that EHEC O157:H7-induced translocation of host proteins to lipid rafts was dependent on intact lipid raft microdomains, pretreatment of cells with M β CD (10 mM) was used to deplete cholesterol and thereby disrupt lipid rafts.²⁰ Cells subjected to M β CD pretreatment failed to recruit PI3K to lipid rafts in response to EHEC O157:H7 (Figure 3b). To verify that M β CD induced disruption of lipid rafts, cholera toxin B subunit staining was performed.²⁵ HEp-2 cells treated with M β CD lacked visible cholera toxin B subunit staining around cells (Figure 3h), compared with untreated cells (Figure 3f). When M β CD-treated cells were rescued with soluble cholesterol, cholera toxin labeling again showed the presence of lipid rafts in the plasma membrane (Figure 3j).

Culture Supernatant and Conditioned Medium Cannot Induce the Recruitment of PI3K to Lipid Rafts

To determine whether bacterial-secreted factors were able to elicit EHEC-induced recruitment of PI3K to lipid microdomains, culture supernatants and conditioned media were collected. Cells treated with culture supernatant and conditioned medium (either filtered or nonfiltered) did not result in the recruitment of PI3K to lipid rafts (Figure 3a and b).

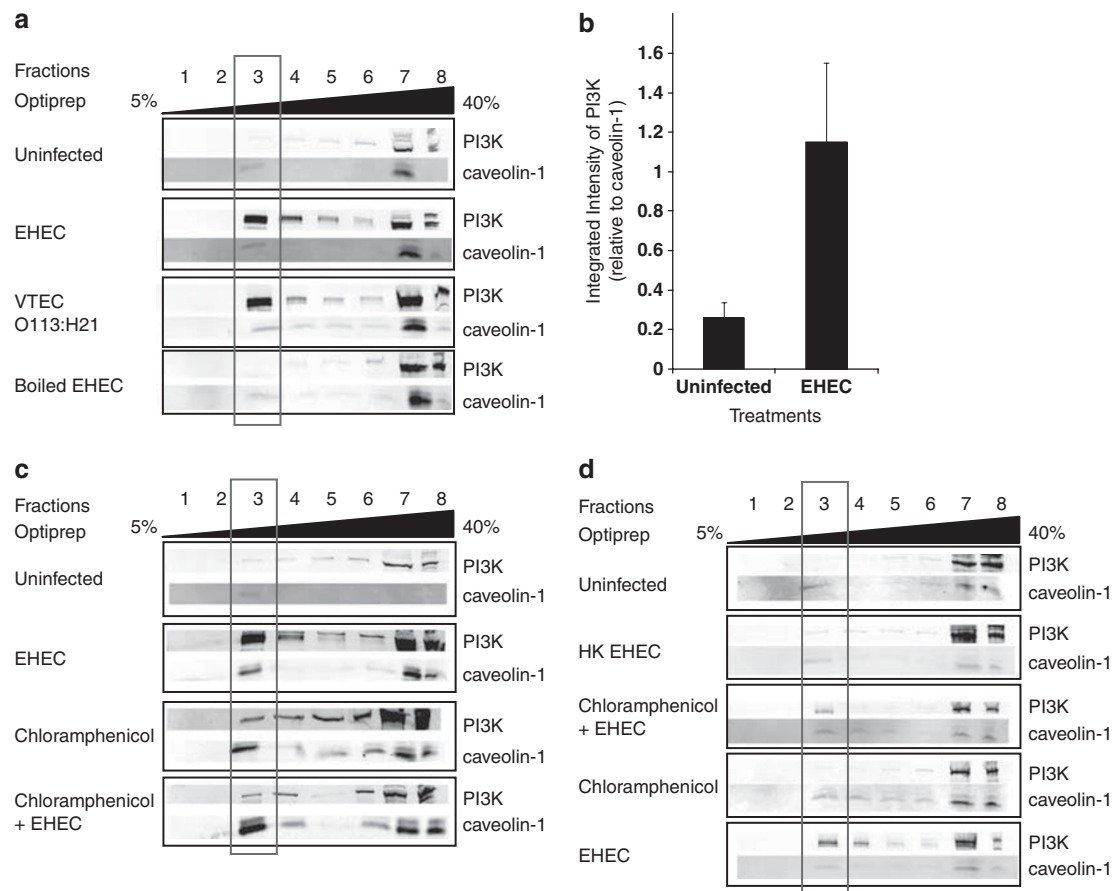


Figure 1 Phosphoinositide 3-kinase (PI3K) is recruited to lipid rafts in response to enterohemorrhagic *Escherichia coli* O157:H7 infection, and newly synthesized bacterial proteins are required for PI3K recruitment to lipid rafts. Western blots of PI3K from ultracentrifugation fractions of whole-cell (HEp-2) extracts. The presence of PI3K in the caveolin-1-containing fraction indicates that it is recruited to lipid rafts in response to bacterial infection. The presence of PI3K in fraction 3 of VTEC O113:H21-infected cells indicate that recruitment is independent of the *eae* gene. The lack of PI3K in fraction 3 of uninfected and boiled EHEC-infected cells shows that recruitment is induced by live bacteria (a). Recruitment was quantified using densitometry and was expressed graphically ($n = 5$, $P < 0.05$) (b). PI3K was not recruited in host cells infected with chloramphenicol-treated EHEC O157:H7, indicating that metabolically active bacteria are required for recruitment of host signaling proteins (c). EHEC-infected Intestine 407 cells also induced translocation of PI3K to lipid rafts (d).

EHEC does not Activate the PI3K/Akt Pathway During Infection

To investigate downstream signals activated in response to EHEC-mediated PI3K recruitment to lipid rafts, whole-cell protein extracts were taken 5 min to 1 h (Figure 3d), and at 3 and 6 h after infection (Figure 3c). The amount of phospho-Akt was determined by western blotting. Although PI3K was recruited to detergent-insoluble microdomains in response to EHEC infection, phosphorylation of Akt, which is a common downstream effector,³⁴ was not detected.

Delayed Colonization of NPC Colonic Mucosa by *C. rodentium*

To extend these findings to an *in vivo* setting, wild-type BALB/c and NPC^{-/-} mice were used. BALB/c and NPC^{-/-} mice were infected orogastrically with the murine-specific AE bacterium, *C. rodentium*.³⁵ In all mice, *C. rodentium* was recovered by rectal swabbing starting at day 3 after orogastric challenge until the end of the infection protocol, indicating

that the organism was able to successfully colonize and infect both wild-type and NPC^{-/-} mice. Six days after challenge, there was a homogeneous bacterial adherence pattern on the colonic mucosa in infected BALB/c mice (Figure 4b). By contrast, there was minimal *C. rodentium* adherence detected on the colonic surface of NPC^{-/-} mice at 6 days after infection (Figure 4e). Furthermore, a more homogeneous pattern of bacterial adherence was detected in NPC^{-/-} mice at 12 days after infection (Figure 4f). At this time, adherent bacteria were largely cleared from the mucosa of wild-type, *C. rodentium*-infected mice.

C. rodentium-Induced AE Lesions are Delayed in NPC^{-/-} Mice

Segments of the distal colon were assessed by transmission electron microscopy for the presence of AE lesions, characteristic of adherent *C. rodentium*.¹⁰ In contrast to uninfected mice, which showed intact apical microvilli on columnar epithelia (Figure 5a), wild-type mice challenged

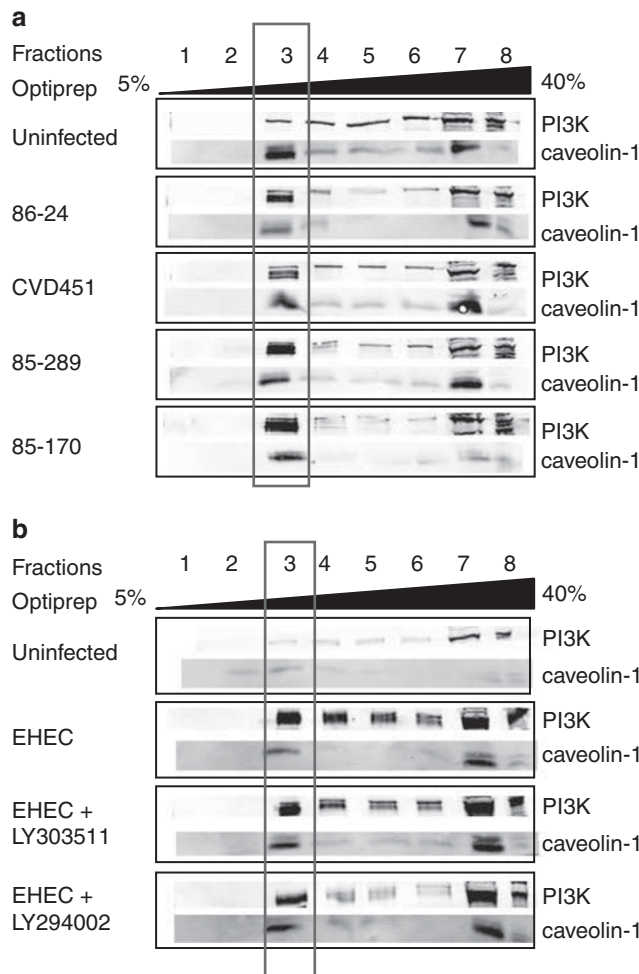


Figure 2 Activated phosphoinositide 3-kinase (PI3K) is recruited to lipid rafts in response to infection, independent of the type III secretion system and Shiga-like toxins 1 and 2. Western blots of PI3K from ultracentrifugation fractions of whole-cell (HEp-2) extracts. PI3K recruitment in EHEC mutant (CVD 451 and 85-170)-infected cells indicates that signaling is independent of the type III secretion system and Shiga-like toxins 1 and 2 (**a**). Cells treated with the PI3K inhibitor LY294002 before EHEC O157:H7 infection had reduced amounts of PI3K recruited to lipid rafts, compared with the amount of PI3K recruited in cells treated with the inactive analog, LY303511, before EHEC infection (**b**).

with *C. rodentium* for 6 days had large numbers of intimately adherent bacteria with typical actin-enriched adhesion pedestals (Figure 5b), but by 12 days after inoculation, AE lesions were no longer observed (Figure 5c). In contrast, AE lesions were not detected in NPC^{-/-} mice at 6 days after infection (Figure 5d and e). Intimate bacterial adherence and adhesion pedestal formation was evident in NPC^{-/-} mice only after 12 days following *C. rodentium* infection (Figure 5f).

C. rodentium-Infected NPC^{-/-} Mice Show Reduced Colonic Epithelial Cell Hyperplasia

Compared with uninfected mice (Figure 6a), histological sections obtained from wild-type mice showed an increase in thickness of the colonic epithelium at both 6 (Figure 6b) and

12 days (Figure 6c) after *C. rodentium* challenge. In contrast, NPC^{-/-} mice had a reduction in hyperplasia of the colonic mucosa in response to *C. rodentium* infection at 12 days (Figure 6d–g).

The reduction in mucosal thickness of *C. rodentium*-infected NPC^{-/-} mice compared with BALB/c mice could be because of either increased cell death or reduced cellular proliferation. Histological sections of *C. rodentium*-infected wild-type and NPC^{-/-} colonic tissue assessed by TUNEL assay showed no differences in surface epithelial cell apoptosis (data not shown). However, colonocyte proliferation, assessed through BrdU staining in infected wild-type mice, showed an increase in both the number of mitotic cells and the size of the proliferation zone at both 6 (Figure 7b) and 12 days (Figure 7c) after infection compared with uninfected mice (Figure 7a). Colonocyte proliferation was maximal at day 6 after infection in wild-type mice. In contrast to wild-type mice, *C. rodentium* infection of NPC^{-/-} mice resulted in only moderate increases in epithelial cell mitosis at both 6 and 12 days after infectious challenge, when maximal bacterial colonization was present (Figure 7e and f, respectively). These changes were quantified as increases in the zone of proliferation – the maximal height of BrdU-labeled cells from the base of well-oriented crypts (Figure 7g).

NPC^{-/-} Mice Produce Reduced Levels of the Proinflammatory Cytokine IFN- γ in Response to *C. rodentium* Infection

Epithelial hyperplasia and colonic mucosal inflammation in *C. rodentium* infection is analogous to enteric immunopathological conditions in patients, such as chronic inflammatory bowel disease.¹⁰ Multiple proinflammatory cytokines are elicited in response to *C. rodentium* infection.^{36,37} Therefore, to assess the adaptive immune responses elicited, splenocytes were isolated from uninfected and *C. rodentium*-challenged BALB/c and NPC^{-/-} mice. Isolated splenocytes were stimulated *in vitro* with *C. rodentium* sonicate and then IFN- γ and IL-10 levels were measured as representative of Th1 and T_{regulatory} cytokine responses, respectively.²⁷ As shown in Figure 8a, wild-type mice showed a proinflammatory, Th1-predominant cytokine response 12 days after *C. rodentium* exposure. By contrast, infected NPC^{-/-} mice had a reduced IFN- γ response. This response may be regulated by an increased T_{regulatory} response, because higher levels of IL-10 were present in splenocytes derived from NPC^{-/-} mice at both 6 and 12 days after infection, compared with wild-type mice challenged with *C. rodentium* (Figure 8b).

DISCUSSION

Multiple signaling molecules have a role in orchestrating host cell responses to EHEC infection,²¹ leading to the development of mucosal inflammation,³⁸ cytoskeleton rearrangements,³⁹ and disruption of intercellular tight junctions.⁴⁰ PI3K, a lipid kinase, catalyzes the production of

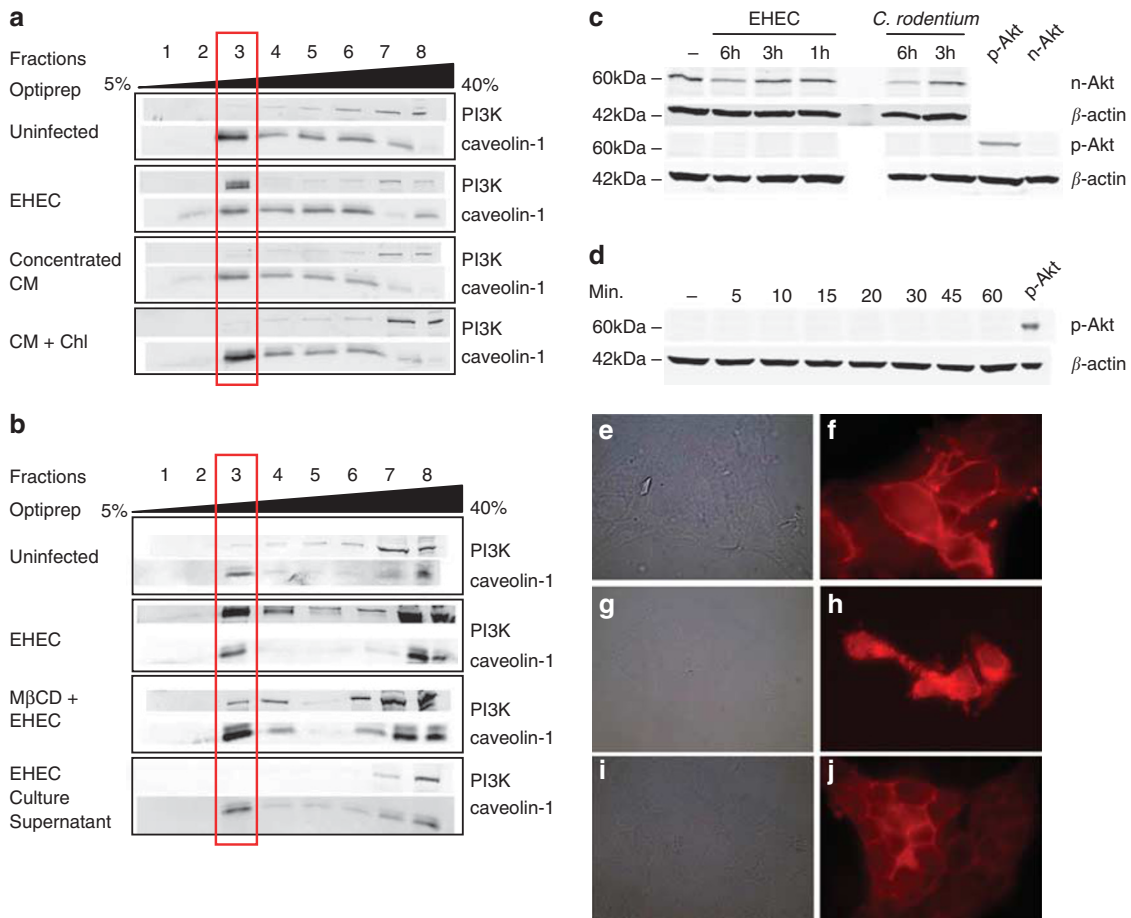


Figure 3 Intact lipid microdomains are required for EHEC-induced translocation of phosphoinositide 3-kinase (PI3K) to lipid rafts, whereas secreted bacterial factors are insufficient to induce this recruitment. Conditioned medium did not induce the recruitment of PI3K to lipid microdomains on host cell membranes (**a**). Disruption of lipid rafts by depleting cellular cholesterol using MβCD (10 mM) leads to decreased recruitment of the host signaling protein, PI3K, in response to EHEC O157:H7 infection. Culture supernatant alone was unable to induce recruitment of PI3K (**b**). Phosphorylation of the PI3K downstream effector Akt was not detected in response to EHEC and *C. rodentium* infections (**c, d**), suggesting an alternative activated pathway. Lipid raft disruption after cholesterol-depleting MβCD treatment was visualized using Alexa fluor 594-labeled cholera toxin subunit B: untreated cells (**e** and **f**), MβCD-treated cells (**g, h**), and MβCD-treated epithelia replenished with soluble cholesterol (**i, j**).

membrane-bound lipid second messengers after stimulation through tyrosine kinases, cytokine receptors, and integrin receptors.⁴¹ In response to pathogen infections, PI3K regulates cytoskeleton rearrangements following both bacterial adhesion⁴² and invasion⁴³ of other bacterial pathogens. However, the mechanisms by which EHEC modulates host signal transduction pathways are still largely unknown.

Akt, also known as PKB, is a key regulator of host cell survival by inhibiting apoptosis, control of the cell cycle and various proinflammatory responses, including the activation of the transcription factor NFκB. Akt is activated downstream of PI3K.⁴⁴ Many bacterial effector proteins trigger the Akt pathway to manipulate host cell function leading to increased adherence and invasion and inducing cytoskeletal rearrangements.⁴⁵ However, in our studies, phosphorylation of Akt was not detected in response to EHEC infection, supporting previous findings that EHEC infection inhibits

activation of the Akt/NFκB signaling cascade.⁴⁶ Recruitment of PI3K to lipid rafts likely stimulates alternate signaling pathways, such as small GTP-binding proteins, leading to pedestal formation in the apical cytoplasm beneath intimately adherent AE organisms.⁴⁷

The characteristic AE lesions seen in eukaryotic cells after noninvasive EHEC O157:H7 infection involves the presence of intact specialized lipid microdomains.²⁰ We show, for the first time, using antibody against two closely related PI3K p85 subunits (α and β)⁴⁸ that EHEC hijacks epithelial cell membrane lipid microdomains to recruit the second messenger PI3K. Such a recruitment was not the result of external bacterial surface structures, because PI3K recruitment to lipid rafts was only observed when cells were infected with live microorganism and not when using heat-killed bacteria.

Recruitment of PI3K to lipid rafts was observed when epithelial cell monolayers were infected with EHEC strain

CVD-451, a type III secretion mutant; indicating that PI3K recruitment to lipid rafts is mediated by a nontype III secretion system bacterial effector.⁴⁹ This recruitment may be induced by secreted bacterial effectors localized in detergent-resistant microdomains with the ability to recruit SH2/3 ligands, leading to pedestal formation. This has been

shown previously, for example, when using Tir derived from an enteropathogenic *E. coli* strain.⁵⁰

Cells infected with chloramphenicol-treated bacteria to block prokaryotic protein synthesis¹⁸ reduced the recruitment of PI3K to lipid rafts during the infectious process. This finding indicates that new bacterial protein(s) secreted

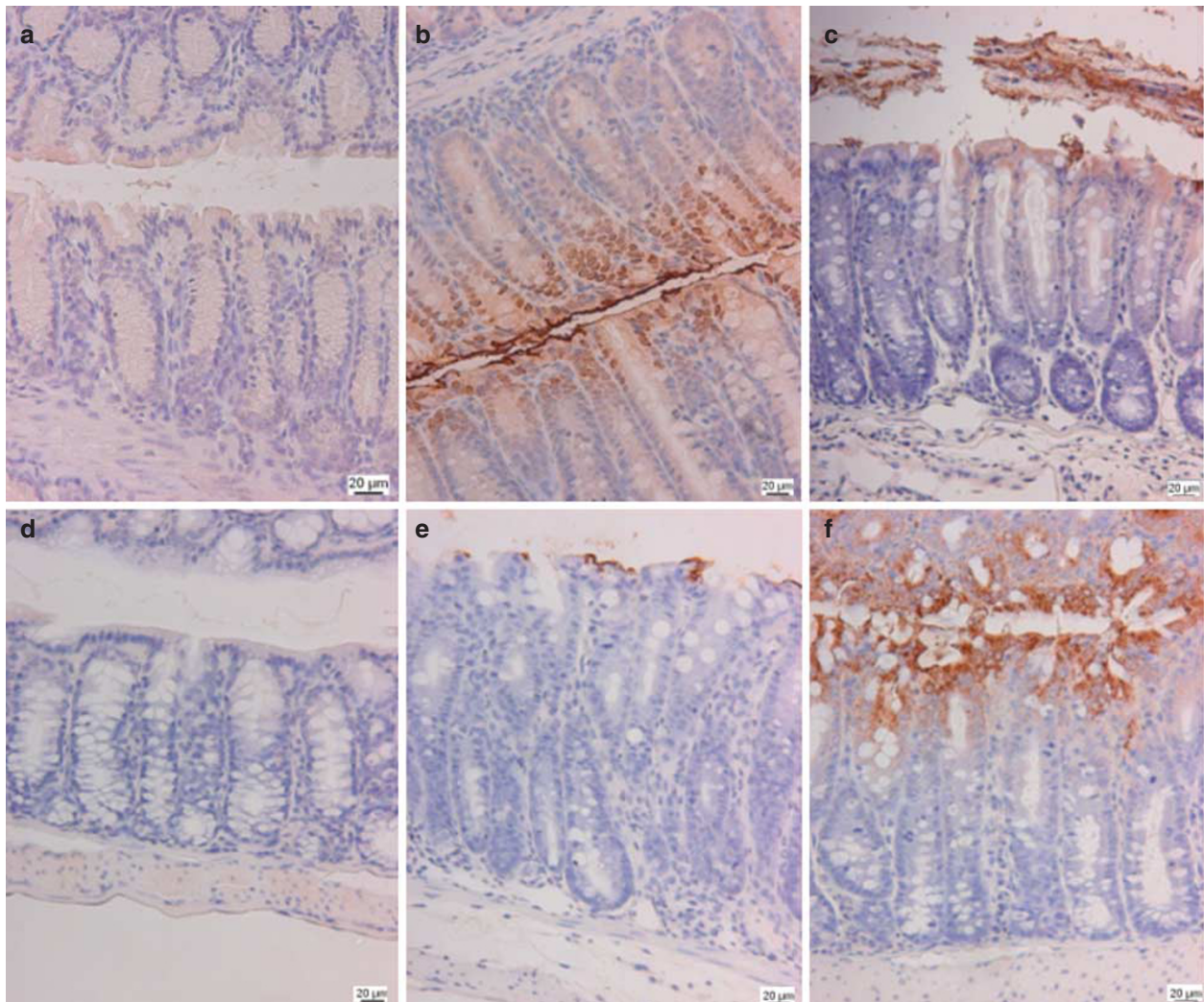
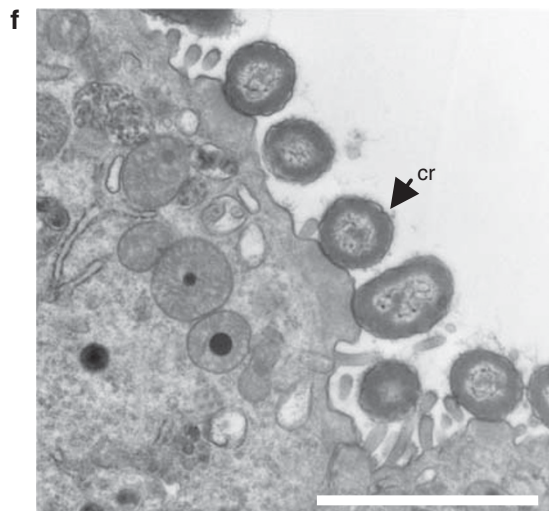
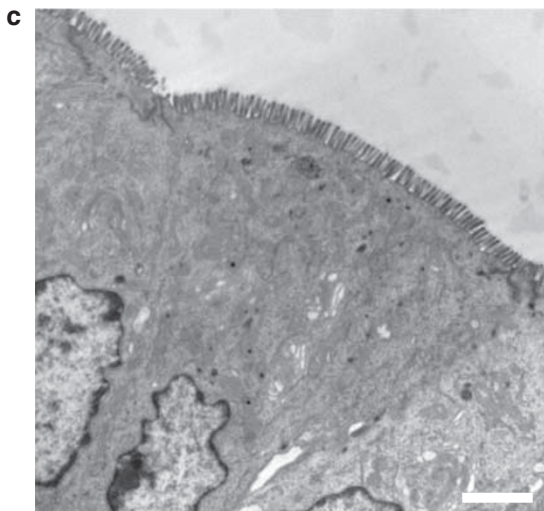
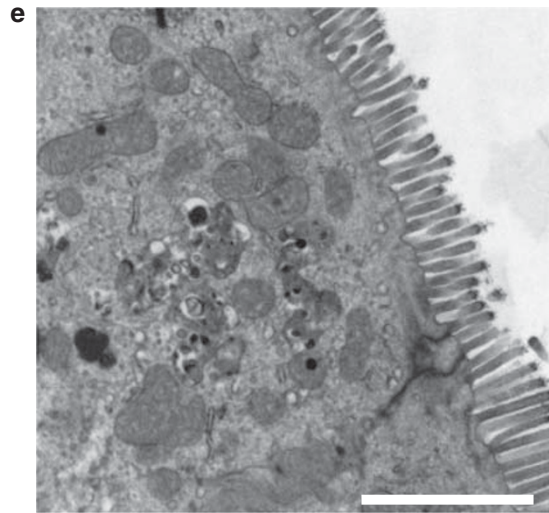
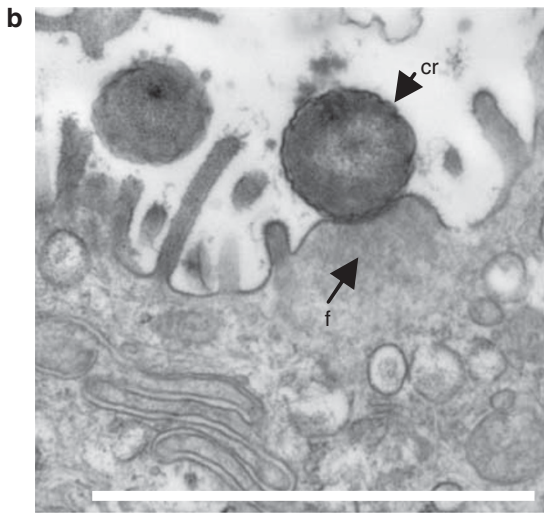
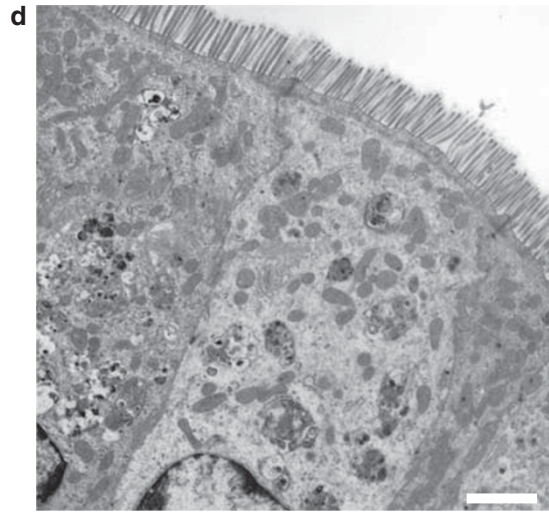
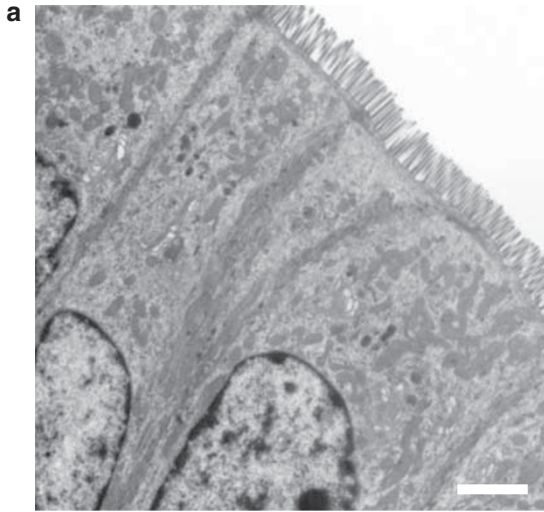


Figure 4 *Citrobacter rodentium* colonization is delayed in the colonic mucosa of NPC^{-/-} mice. Immunohistochemistry of colonic mucosa stained with antibody against *C. rodentium*. Uninfected wild-type BALB/c (a). Wild-type BALB/c mice infected for 6 days show a thick band of *C. rodentium* adherent along the apical aspect of the luminal mucosa (b). Wild-type BALB/c mice infected for 12 days showed *C. rodentium* staining of luminal contents and few adherent bacteria (c). Uninfected NPC^{-/-} mouse colon (d). *C. rodentium*-infected NPC^{-/-} colonic sections obtained 6 days after infectious challenge show a few patches of adherent bacteria (e). NPC^{-/-} tissues obtained from colons 12 days after infection showed *C. rodentium* binding to mucosal surfaces of colonocytes (f). Approximate original magnifications for each photomicrograph, $\times 200$.

Figure 5 Attaching–effacing (AE) lesions induced by *Citrobacter rodentium* infection are delayed in NPC^{-/-} mice. Transmission electron photomicrographs of distal colonic mucosa of uninfected BALB/c columnar epithelium with an intact brush border (a). Higher magnification of an AE lesion-producing *C. rodentium* bacterium (cr) on a BALB/c colonocyte 6 days after inoculation (b). The AE lesion shows characteristic effacement of the brush border microvilli at the site of intimate bacterial adherence and an F-actin-enriched pedestal underlying the adherent bacterium. BALB/c mice colonic tissue obtained 12 days after infectious challenge was devoid of AE lesions (c). Uninfected NPC mouse tissue (d). NPC^{-/-} mouse colon collected 6 days after *C. rodentium* orogastric inoculation lacked AE lesions (e). Bound *C. rodentium* (cr) to an NPC^{-/-} colonocyte 12 days after challenge forms AE lesions (f). Bars = 2 μ m.



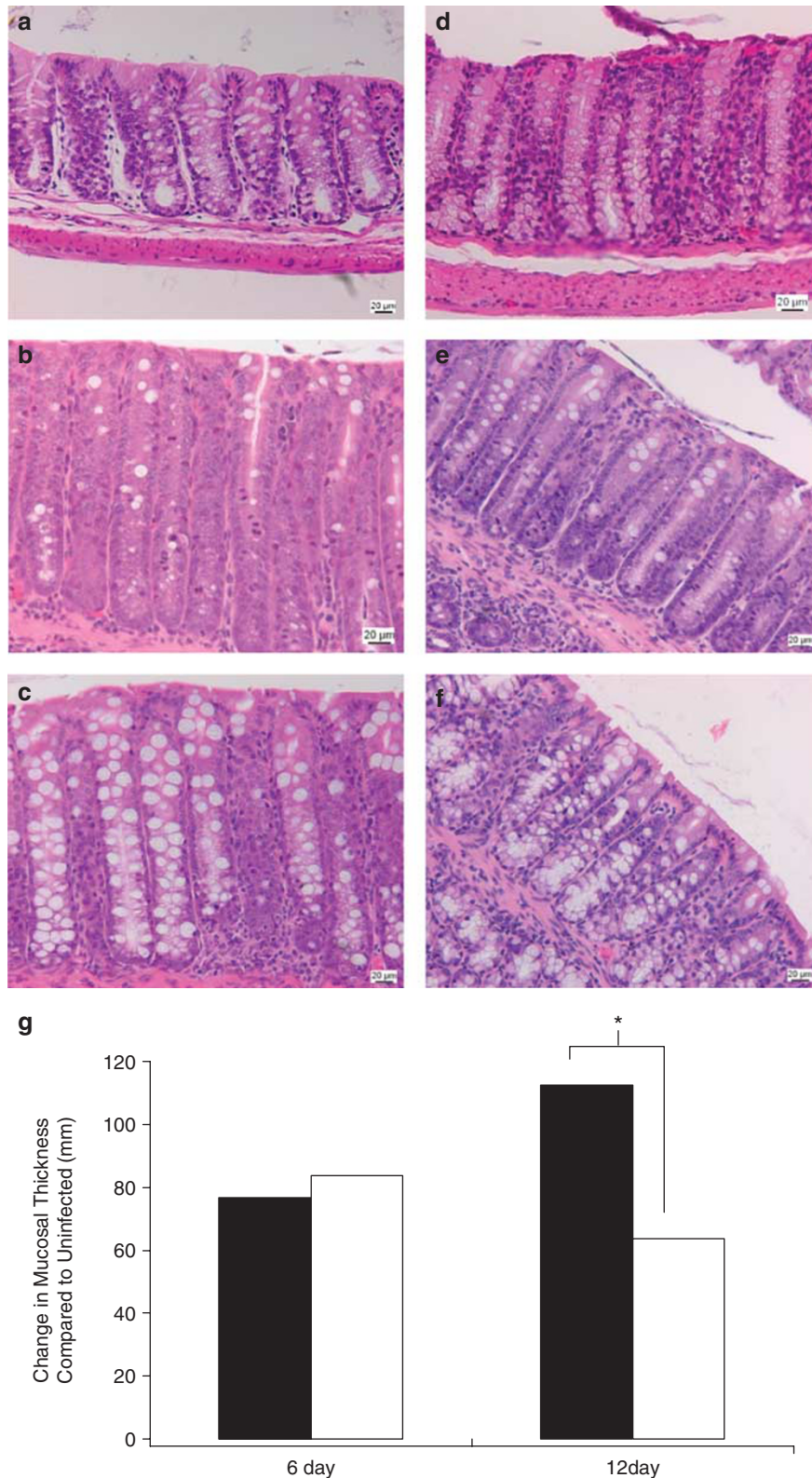


Figure 6 *Citrobacter rodentium*-induced epithelial cell hyperplasia is reduced in NPC^{-/-} mice. Photomicrographs of representative colonic sections showing increases in crypt length in response to *C. rodentium* infection. Uninfected BALB/c (a), 6-day-infected BALB/c (b), 12-day-infected BALB/c (c), Uninfected NPC^{-/-} (d), 6-day-infected NPC^{-/-} (e), 12-day-infected NPC^{-/-} (f). Original magnification for all photomicrographs × 200. Increases in crypt length over uninfected baseline values were quantified (g). A difference in the change in crypt length was observed at 12 days after infection (64 ± 8.251 μm vs 112 ± 2.958 μm; *P < 0.05), but not at 6 days after infection. BALB/c = black bars, NPC^{-/-} = white bars.

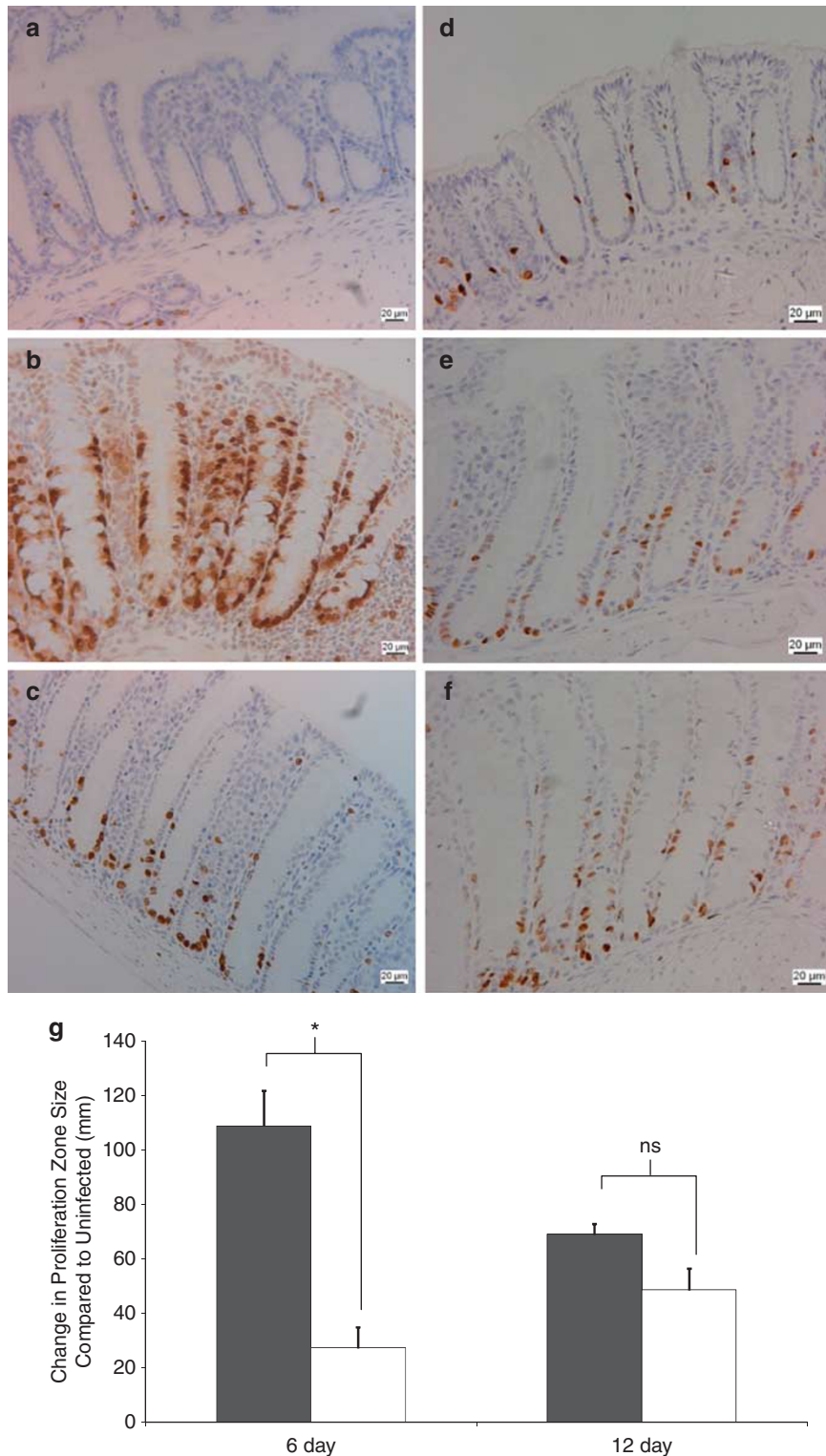


Figure 7 Colonocyte proliferation is reduced in NPC^{-/-} mice infected with *Citrobacter rodentium*. Photomicrographs of colonic sections showing proliferating colonocytes through incorporation of BrdU during mitosis. Uninfected BALB/c crypts show few BrdU-positive dividing colonocytes (a). Large numbers of BrdU-positive colonocytes are observed in BALB/c tissue sections 6 days (b) and 12 days (c) after infection. Uninfected NPC^{-/-} crypts showed few proliferating cells (d), and NPC^{-/-} colonic sections both 6 days (e) and 12 days (f) after infection had just a moderate increase in the number of BrdU-positive cells. Approximate original magnification for each photomicrograph, $\times 200$. The size of the zone of proliferation was quantified and expressed as the change in zone size over the uninfected baseline (g). Proliferation was maximal in BALB/c mice 6 days after infection (71 ± 26.3 pg/ml vs 17.6 ± 17.6 pg/ml, $*P < 0.001$). No differences were observed between BALB/c and NPC^{-/-} mice 12 days after infection. BALB/c = black bars, NPC^{-/-} = white bars.

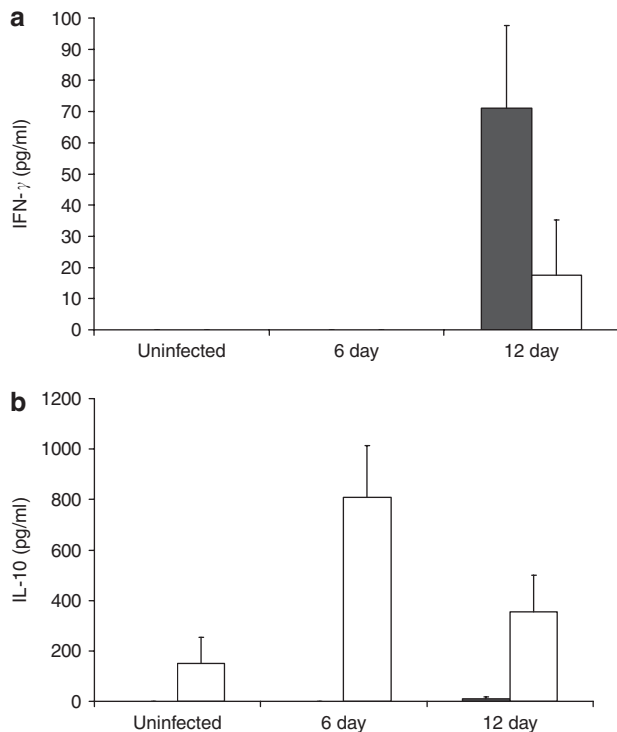


Figure 8 Altered cytokine profiles in NPC^{-/-} mice infected with *Citrobacter rodentium*. Cytokine profiles of splenocytes isolated from uninfected and *C. rodentium*-challenged BALB/c (black bars) and NPC^{-/-} (white bars) mice incubated with *C. rodentium* sonicates. IFN- γ secretion 12 days after infection was reduced in NPC^{-/-} mice ($P < 0.05$) (a). Anti-inflammatory cytokine IL-10 secretion was increased at both 6 ($P < 0.001$) and 12 days ($P < 0.05$) after *C. rodentium* infection of NPC^{-/-} mice (b).

into the culture medium triggers the recruitment of PI3K to cholesterol-enriched microdomains in the host cell plasma membrane. However, secreted bacterial factors alone (using conditioned medium collected from host–bacteria cocultures) did not induce the recruitment of PI3K to lipid rafts. Therefore, bacterial attachment to the cell monolayer is required. Such contact-dependent effects have been described previously.⁴⁰

Although production of Shiga toxins is reported to promote bacterial colonization in the human intestine,⁵¹ the ability of EHEC O157:H7 to elaborate Shiga toxins does not have a role in recruiting PI3K to lipid rafts.⁵² The reduction in EHEC-induced PI3K recruitment to lipid rafts in the presence of a specific pharmacological inhibitor against PI3K suggests that an activated protein was recruited. Such a recruitment is most likely the first step that leads to epithelial barrier disruption and reorganization of the host cell cytoskeleton.

Previous studies have shown that the presence of cholesterol-enriched plasma membrane microdomains *in vitro* is required for adherence and pedestal formation by AE *E. coli*.^{11,20} When lipid rafts are disrupted with the cholesterol-sequestering reagent, M β CD, EHEC no longer induces the translocation of PI3K to lipid rafts. The presence of

caveolin-1 in low-density fraction even after M β CD treatment is likely because of an uneven distribution of caveolin-1 in caveolae present on the basolateral aspect of the plasma membrane and in membranes surrounding intracellular organelles.⁵³ An alternative explanation is that cholesterol is more readily removed from nonmicrodomain regions than from the liquid-ordered phase in which it is more tightly packed and less easily extracted by agents such as M β CD.⁵⁴

The interaction of microbial pathogens with host cell membrane cholesterol and lipid rafts has become a major theme of interest in disease pathogenesis.^{55,56} Previous *in vitro* studies show that multiple bacteria, including *Salmonella*,⁵⁷ *Shigella*,⁵⁸ *Brucella*,⁵⁹ and *E. coli*,^{11,20,60} interact with these cholesterol-enriched microdomains. However, the molecular mechanisms underlying these interactions are still largely undefined. Direct interactions of bacterial proteins with host lipid rafts have been described. For example, type III secretion system bacterial effectors from *Salmonella* PipB⁶¹ and EPEC Tir¹¹ are targeted to lipid rafts, whereas *Salmonella* SipB and *Shigella* IpaB are cholesterol-binding proteins.⁶²

We showed previously that depletion of cellular cholesterol decreases intimate attachment of AE *E. coli*.²⁰ AE lesions were restored when cells are allowed to recover cholesterol.²⁰ These findings were confirmed using primary fibroblasts harboring a defect in the Niemann–Pick C 1 (NPC1) gene.²⁰ Niemann–Pick type C disease is a cholesterol storage disorder resulting in neurodegeneration.⁶³ Mutations in *npc1* and *npc2* result in aberrant lipid transport,^{64,65} which results in decreased lipid rafts and lipid raft-associated markers on the plasma membrane of affected cells.⁶⁶ Taken together, these findings suggest that lipid rafts are required for AE lesion formation in response to EHEC O157:H7 and *C. rodentium* infection *in vitro*. Using a series of pharmacological inhibitors, we previously identified that host enzymes, including phospholipase C- γ (PLC- γ) and PI3K, are involved in the signal transduction cascades that lead to cytoskeletal rearrangements.²¹

In this study, we describe the importance of cholesterol during host–pathogen interactions of the mouse pathogen *C. rodentium* *in vivo*. To our knowledge, this is the first *in vivo* study confirming an interaction between host cholesterol-enriched microdomains and an AE noninvasive enteric bacterial pathogen. Although *C. rodentium* infection of wild-type BALB/c mice resulted in AE lesion formation maximally at 6 days after infection, *C. rodentium*-induced lesions in NPC^{-/-} mice were found later during the infection period, at 12 days. This difference is likely because of the inability of *C. rodentium* to bind and colonize NPC^{-/-} colonic mucosa, despite similar shedding patterns in BALB/c and NPC^{-/-} mice. Maximum colonization occurred on days 6 and 10 after infection in wild-type mice and was decreased by postinfection day 15 with resolution of disease. Such a recovery was not observed in NPC mice infected with *C. rodentium*. Colonization data suggest that there could be a

secondary, alternative binding mechanism for *C. rodentium* to attach to the colonic mucosa. Partitioning of PI3K into cholesterol-rich microdomains is necessary, but not sufficient, to induce AE lesions.

Adherence of *C. rodentium* to colonocytes correlated with maximal responses in cellular proliferation. The time-dependent binding could delay *C. rodentium* pathogenesis in the NPC^{-/-} mouse, resulting in a less-severe colonic epithelial cell hyperplasia response, compared with infection in wild-type mice. Colonization and binding of *C. rodentium* to mucosal surfaces require multiple factors. Initial adhesion of the bacterium to host cells is believed to be accomplished by the colonization factor Citrobacter (CFC) type IV pilus.⁶⁷ After initial adherence, AE pathogens secrete Tir directly into the host plasma membrane. Tir mutants are unable to colonize wild-type mice and do not cause disease.⁶⁸ The LEE pathogenicity island locus encodes Tir, an effector protein that has been isolated from lipid rafts.¹¹ Furthermore, the type III secretion system that delivers Tir to the host cell is regulated by lipid rafts,⁶⁹ and utilizes these cholesterol-rich microdomains as targets for pore formation,⁶² thereby allowing for a direct link between the bacterium and host cells. During the normal course of infection, *C. rodentium* colonizes the colon within the first 2–3 days after infection,⁶⁷ and is recovered in fecal samples for no more than a few weeks.⁷⁰ Noncolonizing mutants, by contrast, are cleared within days of inoculation.⁶⁸ Preventing either the initial attachment of *C. rodentium* to host cells or Tir translocation would serve to inhibit the colonization that was observed in NPC^{-/-}-infected mice.

The observation that maximal mitotic responses (incorporation of BrdU) occurred during times of maximal binding of bacteria to colonic surfaces confirms the belief that the hyperplastic response is contact dependent. Thus, reduced adhesion of *C. rodentium* to NPC^{-/-} colonic mucosa may similarly abrogate the epithelial cell hyperplastic response. Current evidence indicates that colonic hyperplasia is dependent on the non-LEE-encoded effector A (NleA, also known as EspI),⁷¹ as *C. rodentium* strains harboring deletions in *nleA* do not result in colonic epithelial cell hyperplasia.⁷²

Reductions in lipid-raft microdomains are also likely to affect type III secretion. Thus, decreased transfer of NleA in NPC^{-/-} mice could well have a role in reducing the proliferative responses in colonocytes. On the other hand, *C. rodentium* infection also results in the production of serine proteases, which activate the proteinase-activated receptor 2 (PAR2).⁷³ Infected mice treated with a serine proteinase inhibitor and PAR2^{-/-} mice show decreased hyperplastic changes in colonic mucosa.²³ Whether PAR2 activation is deficient in NPC^{-/-} cells is not known, but PAR2 signaling is mediated by G-proteins, which are known to associate with lipid-raft microdomains.¹³

Another important factor affecting the development of *C. rodentium*-induced colonic epithelial cell hyperplasia is the host immune system.⁷⁴ *C. rodentium* elicits a distinct

proinflammatory cytokine response characterized by high levels of Th1 cytokines, including IFN- γ and IL-12.³⁶ In this study, there was a decrease in proinflammatory cytokine responses in NPC^{-/-} mice challenged with *C. rodentium*, as well as marked differences in the secreted T_{regulatory} cytokine profile. IL-10 is an anti-inflammatory cytokine that acts to counterbalance proinflammatory signals.^{75,76} Other studies have noted varying effects, with increases in both T_{regulatory} and Th2 cytokines in response to *C. rodentium* infection. Johnson-Henry *et al*²⁷ observed that mice pretreated with probiotics had elevated IL-10 secretion from splenocytes and ameliorated *C. rodentium* disease pathogenesis. By contrast, helminth infection, which elevates Th2 cytokine responses, prevents colitis in noninfectious animal models,^{77,78} but results in an increased severity of disease in response to *C. rodentium* infection.³⁷ A major difference between these outcomes is the ability of *C. rodentium* to bind to the mucosal surface.

Taken together, these complementary *in vitro* and *in vivo* studies of host epithelial cell responses to noninvasive, AE pathogens show the importance of cholesterol-enriched microdomains as signal transduction platforms that mediate signaling between the infecting organism and the cytosol of the host epithelial cell.

ACKNOWLEDGEMENTS

This work was supported by operating grants from the Canadian Institute for Health Research (CIHR). GS-T was the recipient of a CIHR Canada Graduate Scholarship—Master's Award, CIHR Frederick Banting, and Charles Best Canada Graduate Scholarships—Doctoral Award and research training funding support provided by the SickKids Foundation Graduate Scholarships at the University of Toronto. *In vivo* studies were conducted by Jason D Riff, who was supported through a studentship by the Ontario Student Opportunity Trust Fund—Hospital for Sick Children Foundation Student Scholarship Program, and a University of Toronto Fellowship. PMS is the recipient of a Canada Research Chair in Gastrointestinal Disease.

DISCLOSURE/CONFLICT OF INTEREST

The authors declare no conflict of interest.

1. Kaper JB, Nataro JP, Mobley HL. Pathogenic *Escherichia coli*. *Nat Rev Microbiol* 2004;2:123–140.
2. Jandu N, Shen S, Wickham ME, *et al*. Multiple seropathotypes of verotoxin-producing *Escherichia coli* (VTEC) disrupt interferon-gamma-induced tyrosine phosphorylation of signal transducer and activator of transcription (Stat)-1. *Microb Pathog* 2007;42:62–71.
3. Cooley M, Carychao D, Crawford-Miksza L, *et al*. Incidence and tracking of *Escherichia coli* O157:H7 in a major produce production region in California. *PLoS ONE* 2007;2:e1159.
4. Rendon MA, Saldana Z, Erdem AL, *et al*. Commensal and pathogenic *Escherichia coli* use a common pilus adherence factor for epithelial cell colonization. *Proc Natl Acad Sci USA* 2007;104:10637–10642.
5. Nutikka A, Lingwood C. Generation of receptor-active, globotriaosyl ceramide/cholesterol lipid 'rafts' *in vitro*: a new assay to define factors affecting glycosphingolipid receptor activity. *Glycoconj J* 2004;20:33–38.
6. Gobert AP, Vareille M, Glasser AL, *et al*. Shiga toxin produced by enterohemorrhagic *Escherichia coli* inhibits PI3K/NF-kappaB signaling pathway in globotriaosylceramide-3-negative human intestinal epithelial cells. *J Immunol* 2007;178:8168–8174.
7. Gyles CL. Shiga toxin-producing *Escherichia coli*: an overview. *J Anim Sci* 2007;95(13 Suppl):E45–E62.

8. Welinder-Olsson C, Kaijser B. Enterohemorrhagic *Escherichia coli* (EHEC). *Scand J Infect Dis* 2005;37:405–416.
9. Campellone KG, Robbins D, Leong JM. EspFU is a translocated EHEC effector that interacts with Tir and N-WASP and promotes Nck-independent actin assembly. *Dev Cell* 2004;7:217–228.
10. Mundy R, MacDonald TT, Dougan G, *et al.* *Citrobacter rodentium* of mice and man. *Cell Microbiol* 2005;7:1697–1706.
11. Allen-Vercoe E, Waddell B, Livingstone S, *et al.* Enteropathogenic *Escherichia coli* Tir translocation and pedestal formation requires membrane cholesterol in the absence of bundle-forming pili. *Cell Microbiol* 2006;8:613–624.
12. Zobiack N, Rescher U, Laarmann S, *et al.* Cell-surface attachment of pedestal-forming enteropathogenic *E. coli* induces a clustering of raft components and a recruitment of annexin 2. *J Cell Sci* 2002;115 (Part 1):91–98.
13. Simons K, Toomre D. Lipid rafts and signal transduction. *Nat Rev Mol Cell Biol* 2000;1:31–39.
14. Brown DA, London E. Functions of lipid rafts in biological membranes. *Annu Rev Cell Dev Biol* 1998;14:111–136.
15. Fielding CJ, Fielding PE. Membrane cholesterol and the regulation of signal transduction. *Biochem Soc Trans* 2004;32(Part 1):65–69.
16. Laude AJ, Prior IA. Plasma membrane microdomains: organization, function and trafficking. *Mol Membr Biol* 2004;21:193–205.
17. Ceponis PJ, McKay DM, Ching JC, *et al.* Enterohemorrhagic *Escherichia coli* O157:H7 disrupts Stat1-mediated gamma interferon signal transduction in epithelial cells. *Infect Immun* 2003;71:1396–1404.
18. Jandu N, Ceponis PJ, Kato S, *et al.* Conditioned medium from enterohemorrhagic *Escherichia coli*-infected T84 cells inhibits signal transducer and activator of transcription 1 activation by gamma interferon. *Infect Immun* 2006;74:1809–1818.
19. Kilsdonk EP, Yancey PG, Stoudt GW, *et al.* Cellular cholesterol efflux mediated by cyclodextrins. *J Biol Chem* 1995;270:17250–17256.
20. Riff JD, Callahan JW, Sherman PM. Cholesterol-enriched membrane microdomains are required for inducing host cell cytoskeleton rearrangements in response to attaching–effacing *Escherichia coli*. *Infect Immun* 2005;73:7113–7125.
21. Johnson-Henry K, Wallace JL, Basappa NS, *et al.* Inhibition of attaching and effacing lesion formation following enteropathogenic *Escherichia coli* and Shiga toxin-producing *E. coli* infection. *Infect Immun* 2001;69:7152–7158.
22. Schraw W, Li Y, McClain MS, *et al.* Association of *Helicobacter pylori* vacuolating toxin (VacA) with lipid rafts. *J Biol Chem* 2002;277:34642–34650.
23. Song KS, Li S, Okamoto T, *et al.* Co-purification and direct interaction of Ras with caveolin, an integral membrane protein of caveolae microdomains. Detergent-free purification of caveolae microdomains. *J Biol Chem* 1996;271:9690–9697.
24. Macdonald JL, Pike LJ. A simplified method for the preparation of detergent-free lipid rafts. *J Lipid Res* 2005;46:1061–1067.
25. Hatano T, Kubo S, Imai S, *et al.* Leucine-rich repeat kinase 2 associates with lipid rafts. *Hum Mol Genet* 2007;16:678–690.
26. Dennis A, Kudo T, Kruidenier L, *et al.* The p50 subunit of NF-kappaB is critical for *in vivo* clearance of the noninvasive enteric pathogen *Citrobacter rodentium*. *Infect Immun* 2008;76:4978–4988.
27. Johnson-Henry KC, Nadjafi M, Avitzur Y, *et al.* Amelioration of the effects of *Citrobacter rodentium* infection in mice by pretreatment with probiotics. *J Infect Dis* 2005;191:2106–2117.
28. Mogilner JG, Sruogo I, Lurie M, *et al.* Effect of probiotics on intestinal regrowth and bacterial translocation after massive small bowel resection in a rat. *J Pediatr Surg* 2007;42:1365–1371.
29. Kubo M, Li TS, Suzuki R, *et al.* Hypoxic preconditioning increases survival and angiogenic potency of peripheral blood mononuclear cells via oxidative stress resistance. *Am J Physiol Heart Circ Physiol* 2008;294:H590–H595.
30. Jones NL, Day AS, Jennings H, *et al.* Enhanced disease severity in *Helicobacter pylori*-infected mice deficient in Fas signaling. *Infect Immun* 2002;70:2591–2597.
31. Bewick V, Cheek L, Ball J. Statistics review 9: one-way analysis of variance. *Crit Care* 2004;8:130–136.
32. Cole LE, Shirey KA, Barry E, *et al.* Toll-like receptor 2-mediated signaling requirements for Francisella tularensis live vaccine strain infection of murine macrophages. *Infect Immun* 2007;75:4127–4137.
33. Shen S, Mascarenhas M, Rahn K, *et al.* Evidence for a hybrid genomic island in verocytotoxin-producing *Escherichia coli* CL3 (serotype O113:H21) containing segments of EDL933 (serotype O157:H7) O islands 122 and 48. *Infect Immun* 2004;72:1496–1503.
34. Cantley LC. The phosphoinositide 3-kinase pathway. *Science* 2002;296:1655–1657.
35. Borenshtein D, McBee ME, Schauer DB. Utility of the *Citrobacter rodentium* infection model in laboratory mice. *Curr Opin Gastroenterol* 2008;24:32–37.
36. Higgins LM, Frankel G, Douce G, *et al.* *Citrobacter rodentium* infection in mice elicits a mucosal Th1 cytokine response and lesions similar to those in murine inflammatory bowel disease. *Infect Immun* 1999;67:3031–3039.
37. Chen CC, Louie S, McCormick B, *et al.* Concurrent infection with an intestinal helminth parasite impairs host resistance to enteric *Citrobacter rodentium* and enhances *Citrobacter*-induced colitis in mice. *Infect Immun* 2005;73:5468–5481.
38. Ismaili A, Philpott DJ, Dytoc MT, *et al.* Signal transduction responses following adhesion of verocytotoxin-producing *Escherichia coli*. *Infect Immun* 1995;63:3316–3326.
39. Shaner NC, Sanger JW, Sanger JM. Actin and alpha-actinin dynamics in the adhesion and motility of EPEC and EHEC on host cells. *Cell Motil Cytoskeleton* 2005;60:104–120.
40. Philpott DJ, McKay DM, Mak W, *et al.* Signal transduction pathways involved in enterohemorrhagic *Escherichia coli*-induced alterations in T84 epithelial permeability. *Infect Immun* 1998;66:1680–1687.
41. Pizarro-Cerda J, Cossart P. Bacterial adhesion and entry into host cells. *Cell* 2006;124:715–727.
42. Kierbel A, Gassama-Diagne A, Rocha C, *et al.* *Pseudomonas aeruginosa* exploits a PIP3-dependent pathway to transform apical into basolateral membrane. *J Cell Biol* 2007;177:21–27.
43. Kierbel A, Gassama-Diagne A, Mostov K, *et al.* The phosphoinositide-3-kinase-protein kinase B/Akt pathway is critical for *Pseudomonas aeruginosa* strain PAK internalization. *Mol Biol Cell* 2005;16:2577–2585.
44. Wiles TJ, Dhakal BK, Eto DS, *et al.* Inactivation of host Akt/protein kinase B signaling by bacterial pore-forming toxins. *Mol Biol Cell* 2008;19:1427–1438.
45. Edwards JL, Apicella MA. *Neisseria gonorrhoeae* PLD directly interacts with Akt kinase upon infection of primary, human, cervical epithelial cells. *Cell Microbiol* 2006;8:1253–1271.
46. Bosse T, Ehinger J, Czuchra A, *et al.* Cdc42 and phosphoinositide 3-kinase drive Rac-mediated actin polymerization downstream of c-Met in distinct and common pathways. *Mol Cell Biol* 2007;27:6615–6628.
47. Takenouchi H, Kiyokawa N, Taguchi T, *et al.* Shiga toxin binding to globotriaosyl ceramide induces intracellular signals that mediate cytoskeleton remodeling in human renal carcinoma-derived cells. *J Cell Sci* 2004;117(Part 17):3911–3922.
48. Tang CH, Lu DY, Yang RS, *et al.* Leptin-induced IL-6 production is mediated by leptin receptor, insulin receptor substrate-1, phosphatidylinositol 3-kinase, Akt, NF-kappaB, and p300 pathway in microglia. *J Immunol* 2007;179:1292–1302.
49. Guttman JA, Li Y, Wickham ME, *et al.* Attaching and effacing pathogen-induced tight junction disruption *in vivo*. *Cell Microbiol* 2006;8:634–645.
50. Sason H, Milgrom M, Weiss AM, *et al.* Enteropathogenic *Escherichia coli* subverts phosphatidylinositol 4,5-bisphosphate and phosphatidylinositol 3,4,5-trisphosphate upon epithelial cell infection. *Mol Biol Cell* 2009;20:544–555.
51. Robinson CM, Sinclair JF, Smith MJ, *et al.* Shiga toxin of enterohemorrhagic *Escherichia coli* type O157:H7 promotes intestinal colonization. *Proc Natl Acad Sci USA* 2006;103:9667–9672.
52. Proulx F, Seidman EG, Karpman D. Pathogenesis of Shiga toxin-associated hemolytic uremic syndrome. *Pediatr Res* 2001;50:163–171.
53. Absi M, Burnham MP, Weston AH, *et al.* Effects of methyl beta-cyclodextrin on EDHF responses in pig and rat arteries; association between SK(Ca) channels and caveolin-rich domains. *Br J Pharmacol* 2007;151:332–340.
54. Marbeuf-Gueye C, Stierle V, Sudwan P, *et al.* Perturbation of membrane microdomains in GLC4 multidrug-resistant lung cancer cells—modification of ABC1 (MRP1) localization and functionality. *FEBS J* 2007;274:1470–1480.

55. Goluszko P, Nowicki B. Membrane cholesterol: a crucial molecule affecting interactions of microbial pathogens with mammalian cells. *Infect Immun* 2005;73:7791–7796.
56. Lafont F, van der Goot FG. Bacterial invasion via lipid rafts. *Cell Microbiol* 2005;7:613–620.
57. Catron DM, Sylvester MD, Lange Y, *et al*. The salmonella-containing vacuole is a major site of intracellular cholesterol accumulation and recruits the GPI-anchored protein CD55. *Cell Microbiol* 2002;4:315–328.
58. Lafont F, Tran Van Nhieu G, Hanada K, *et al*. Initial steps of Shigella infection depend on the cholesterol/sphingolipid raft-mediated CD44-IpaB interaction. *EMBO J* 2002;21:4449–4457.
59. Watarai M, Makino S, Michikawa M, *et al*. Macrophage plasma membrane cholesterol contributes to Brucella abortus infection of mice. *Infect Immun* 2002;70:4818–4825.
60. Kansau I, Berger C, Hospital M, *et al*. Zipper-like internalization of Dr-positive *Escherichia coli* by epithelial cells is preceded by an adhesin-induced mobilization of raft-associated molecules in the initial step of adhesion. *Infect Immun* 2004;72:3733–3742.
61. Knodler LA, Vallance BA, Hensel M, *et al*. Salmonella type III effectors PipB and PipB2 are targeted to detergent-resistant microdomains on internal host cell membranes. *Mol Microbiol* 2003;49:685–704.
62. Hayward RD, Cain RJ, McGhie EJ, *et al*. Cholesterol binding by the bacterial type III translocon is essential for virulence effector delivery into mammalian cells. *Mol Microbiol* 2005;56:590–603.
63. Chang TY, Reid PC, Sugii S, *et al*. Niemann–Pick type C disease and intracellular cholesterol trafficking. *J Biol Chem* 2005;280:20917–20920.
64. Liscum L, Sturley SL. Intracellular trafficking of Niemann–Pick C proteins 1 and 2: obligate components of subcellular lipid transport. *Biochim Biophys Acta* 2004;1685:22–27.
65. Mukherjee S, Maxfield FR. Lipid and cholesterol trafficking in NPC. *Biochim Biophys Acta* 2004;1685:28–37.
66. Garver WS, Krishnan K, Gallagos JR, *et al*. Niemann–Pick C1 protein regulates cholesterol transport to the trans-Golgi network and plasma membrane caveolae. *J Lipid Res* 2002;43:579–589.
67. Mundy R, Pickard D, Wilson RK, *et al*. Identification of a novel type IV pilus gene cluster required for gastrointestinal colonization of *Citrobacter rodentium*. *Mol Microbiol* 2003;48:795–809.
68. Schauer DB, Falkow S. The eae gene of *Citrobacter freundii* biotype 4280 is necessary for colonization in transmissible murine colonic hyperplasia. *Infect Immun* 1993;61:4654–4661.
69. van der Goot FG, Tran van Nhieu G, Allaoui A, *et al*. Rafts can trigger contact-mediated secretion of bacterial effectors via a lipid-based mechanism. *J Biol Chem* 2004;279:47792–47798.
70. Wiles S, Clare S, Harker J, *et al*. Organ specificity, colonization and clearance dynamics *in vivo* following oral challenges with the murine pathogen *Citrobacter rodentium*. *Cell Microbiol* 2004;6:963–972.
71. Gruenheid S, Sekirov I, Thomas NA, *et al*. Identification and characterization of NleA, a non-LEE-encoded type III translocated virulence factor of enterohaemorrhagic *Escherichia coli* O157:H7. *Mol Microbiol* 2004;51:1233–1249.
72. Mundy R, Petrovska L, Smollett K, *et al*. Identification of a novel *Citrobacter rodentium* type III secreted protein, Espl, and roles of this and other secreted proteins in infection. *Infect Immun* 2004;72:2288–2302.
73. Hansen KK, Sherman PM, Cellars L, *et al*. A major role for proteolytic activity and proteinase-activated receptor-2 in the pathogenesis of infectious colitis. *Proc Natl Acad Sci USA* 2005;102:8363–8368.
74. Artis D, Potten CS, Else KJ, *et al*. Trichuris muris: host intestinal epithelial cell hyperproliferation during chronic infection is regulated by interferon-gamma. *Exp Parasitol* 1999;92:144–153.
75. O'Garra A, Vieira PL, Vieira P, *et al*. IL-10-producing and naturally occurring CD4+ Tregs: limiting collateral damage. *J Clin Invest* 2004;114:1372–1378.
76. Powrie F. Immune regulation in the intestine: a balancing act between effector and regulatory T cell responses. *Ann N Y Acad Sci* 2004;1029:132–141.
77. McKay DM. The beneficial helminth parasite? *Parasitology* 2006;132(Part 1):1–12.
78. Reardon C, Sanchez A, Hogaboam CM, *et al*. Tapeworm infection reduces epithelial ion transport abnormalities in murine dextran sulfate sodium-induced colitis. *Infect Immun* 2001;69:4417–4423.